

# 푸쉬풀 퀀텀 직렬공진형 정류기의 3레벨 예측형 역률개선 기법

문건우, 백인철, 정영석, 이준영, 윤명중  
한국과학기술원 전기 및 전자공학과

## Three-Level Predictive Power Factor Correction Technique for Push-Pull Quantum Series Resonant Rectifier

Gun-Woo Moon, In-Chul Baik, Young-Seok Jung, Jung-Wook Roh, and Myung-Joong Yoon

Department of Electrical Engineering  
Korea Advanced Institute of Science & Technology

**Abstract:** A new three-level push-pull type quantum series resonant rectifier for the power factor correction is proposed. The proposed single phase rectifier enables a zero-current switching operation of all the power devices allowing the circuit to operate at high switching frequencies and high power levels. With the proposed control technique, an unity power factor and greatly reduced line current harmonics can be obtained.

### 1 Introduction

In recent years, due to the power factor correction(PFC) requirement, The conventional PWM boost rectifier operating in continuous current mode for power factor correction is the best way because it has the continuous line current, smallest choke, minimum current distortion and lowest current stress than others [1-4]. However, operation in continuous mode is accompanied with a current and voltage spike due to a hard switching. This increase switching loss and the level of EMI, thus, operational frequency and power density are limited. Recently a predictive current controlled series resonant high power factor rectifier is suggested [5]. This type of converter and control technique can provide zero current switching condition, ease of control, linear characteristics like those of the conventional PWM converters, and reduced line current harmonics. However, a coupled things are still concern. For high power applications, the input filter will become one of the major factors affecting the system cost, volume, and weight. For high voltage applications, high voltage devices have to be used, which produces high conduction losses. With the three-level predictive controlled push-pull quantum series resonant rectifier(PP-QSRR) in this paper, the input filter can be greatly reduced, and the device voltage rating of output side chopper switches is only half of the output voltage.

### 2 Principles of Basic Operation

The basic configuration of three-level PP-QSRR shown in Fig.1 consists of a diode bridge rectifier with the push-pull switches  $P_1$  and  $P_2$ , an isolated resonant power stage, two boost chopper switches  $Q_1$  and  $Q_2$ , and an output filter stage. The push-pull switches  $P_1$  and  $P_2$  are always turned on and off alternatively in synchronization with the zero crossing points of the resonant current. The operation of the PP-QSRR for an unity power factor can be obtained using two boost chopper switches where the switching is

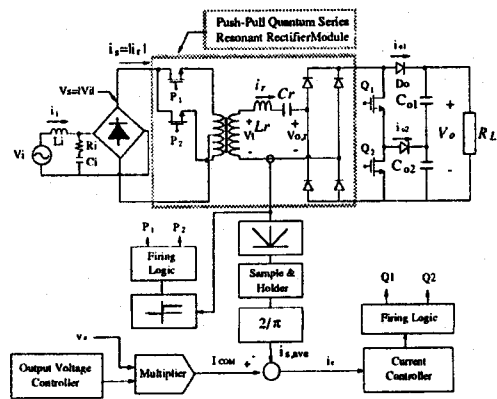


Fig. 1 Circuit Diagram of a Push-Pull Quantum Series Resonant Rectifier.

also occurred at zero crossing points of the resonant current. The amplitude of the resonant current can be rapidly increased with a maximum slope when two switches  $Q_1$  and  $Q_2$  are closed. If  $Q_1$  and  $Q_2$  are open, the output stage is connected in series with the resonant tank circuit and hence the stored energy in the resonant power stage is transferred to the output stage. And if a switch of  $Q_1$  or  $Q_2$  is closed, midimum current slopes are available.

### 3 Sampled Data Dynamic Modeling and Analysis

In order to obtain a simple and effective analytical tool for the analysis, a dynamic model in the discrete time domain is developed. Based on the basic operational principles, the governing equations for the  $k$ -th time event can be derived as follows:

$$V_r(t) = \text{sgn}(i_r(t))V_s(t) = L_r \frac{di_r(t)}{dt} + v_c(t) + V_{o,r}(t) \quad (1a)$$

$$C_r \frac{dv_c(t)}{dt} = i_r(t) \quad (1b)$$

$$(1 - S(k)) | i_r(t) | = C_o \frac{dv_o(t)}{dt} + \frac{1}{R_L} v_o(t) \quad (1c)$$

where  $V_{o,r}(t) = (1 - S(k))\text{sgn}(i_r(t))V_o(t)$  and control variable for  $Q_1$  and  $Q_2$ ,  $S(k)$  has the values of 1, 0.5, and 0. Since the push-pull switches  $P_1$  and  $P_2$  are always turned on and off alternatively, the left hand side of (1a) implies the actual

applied voltage  $V$ , to the resonant tank circuit with respect to the direction of the resonant current. The third term of the right-hand side of (1a),  $V_{o,r}(t)$ , denotes the output voltage reflected to the resonant tank circuit with respect to the control variable  $S(k)$ . Equation (1b) implies the dynamic relation between the resonant capacitor voltage and inductor current, and (1c) denotes the output equation.

The following discrete state equation for a PP-QSRR can be derived as

$$\begin{pmatrix} i_{s,ave}(k+1) \\ v_o(k+1) \end{pmatrix} = \begin{pmatrix} 1-\gamma(1-S(k))(1-S(k+1)) & -\frac{2}{\pi Z}(1-S(k)+(1-\gamma)(1-S(k+1))) \\ \frac{\pi Z \gamma}{2}(1-S(k)) & 1-\gamma \end{pmatrix} \begin{pmatrix} i_{s,ave}(k) \\ v_o(k) \end{pmatrix} + \begin{pmatrix} \frac{4V_s(k)}{\pi Z} \\ 0 \end{pmatrix} \quad (2)$$

Since  $C$ , is chosen as much smaller than  $C_o$ ,  $\gamma$  and  $\dot{\gamma}$  become much smaller than the unity. Therefore, the equation (2) can be simplified as follows:

$$\begin{pmatrix} i_{s,ave}(k+1) \\ v_o(k+1) \end{pmatrix} = \begin{pmatrix} 1 & -\frac{4}{\pi Z}(1-S^*(k+1)) \\ \frac{\pi Z \gamma}{2}(1-S(k)) & 1-\dot{\gamma} \end{pmatrix} \begin{pmatrix} i_{s,ave}(k) \\ v_o(k) \end{pmatrix} + \begin{pmatrix} \frac{4V_s(k)}{\pi Z} \\ 0 \end{pmatrix} \quad (3)$$

where  $S^*(k+1) = (S(k)+S(k+1))/2$ . Note that the average values of the line current  $i_{s,ave}(k+1)$  are directly controlled by moving average of the control variable for a switch  $Q$  that is  $S^*(k+1)$ . The slope of the average rectified resonant current between the  $k$ -th and  $(k+1)$ -th time events,  $Slope(k,k+1)$ , can be easily derived from (3) as follow:

$$\begin{aligned} Slope(k,k+1) &= \frac{i_{s,ave}(k+1) - i_{s,ave}(k)}{(T/2)} \\ &= \frac{8}{\pi Z T} \{V_s(k) - (1-S^*(k+1))V_o(k)\} \\ &= \frac{1}{L_{eq}} \{V_s(k) - (1-S^*(k+1))V_o(k)\}, \end{aligned}$$

where

$$L_{eq} = \left(\frac{\pi}{2}\right)^2 L_r \quad (4)$$

As can be seen in (4), the PP-QSRR module shown in Fig. 1 can be modeled as an equivalent DC inductor  $L_{eq}$  in a proposed sampled data model. Since proposed PP-QSRR is equivalent to conventional boost AC to DC converter, simple characteristics such as ease of control and modeling can be available in the high frequency operation with low switching loss.

#### 4 Three-level predictive Current Control Technique

In this section, a three-level predictive current control technique for a PP-QSRR is developed and the advantages over the previously described current control techniques are discussed. It is noted that the desired control performance can be obtained by selecting the switching status of two switches  $Q_1$  and  $Q_2$  in such a way that the present current error is reduced to be a minimum at the next time event. With this kind of a minimum current error control strategy, the greatly reduced line current harmonics can be expected.

In the following, this control technique is developed step by step using an analytical result from the operational characteristics. Firstly, a control input which can minimize the present current error at the next time event is derived. The present current error is defined as

$$i_e(k) \equiv I_{COM}(k) - i_s(k) \quad (5)$$

where  $I_{COM}(k)$  denotes the desired rectified line current command, which can be obtained from the line voltage divided by a constant  $K$ . The current variation between the  $(k+1)$ -th and  $k$ -th time events can be easily predicted using (4) as follows:

$$i_{s,ave}(k+1) - i_{s,ave}(k) = \frac{4}{\pi Z} \{V_s(k) - (1-S^*(k+1))V_o(k)\} \quad (6)$$

By equating (14) and (15), an ideal control input,  $S_{ideal}^*(k+1)$ , can be easily obtained as

$$S_{ideal}^*(k+1) = 1 - \frac{V_s(k)}{V_o(k)} + \frac{\pi Z}{4V_o(k)} i_e(k) \quad (7)$$

$S_{ideal}^*(k+1)$  is easily implemented by using an analog divider such as AD533. If this ideal control input could be employed at the next sampling time, the current error would always be minimized at the next time event. Since only three values are available in practice for  $S^*(k+1)$ , the final step is to find an actual control variable nearest to the ideal control input for the  $(k+1)$ -th time event. This can be simply

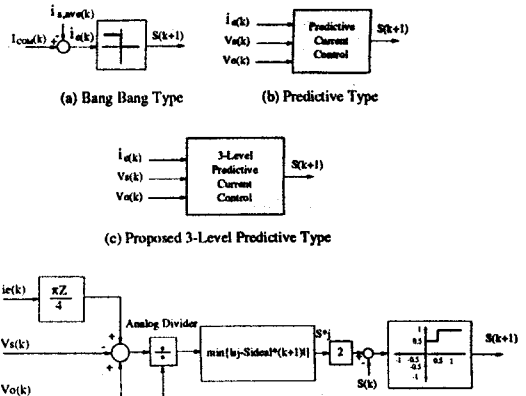


Fig. 2 Simple Block Diagrams of Various Control techniques and Detailed Block Diagram of Three-level Predictive Current Control Technique

implemented by logic circuitry and expressed mathematically as follows:

$$\begin{aligned} S^*(k+1) &= s_j^* = \{s_j \in (1,0.25,0.5,0.75,0)\} \\ &\min_{j \in 1, \dots, 5} \{|s_j - S_{ideal}^*(k+1)|\}. \end{aligned} \quad (8)$$

Finally, the actual switching signal of  $Q$  for  $(k+1)$ -th time event is determined from (4) and (8) as follows:

$$S(k+1) = \begin{pmatrix} 1, & \text{if } \beta > 1 \\ \beta, & \text{if } 0 \leq \beta \leq 1 \\ 0, & \text{if } \beta < 0 \end{pmatrix} \quad (9)$$

where  $\beta = 2s_j^* - S(k)$ . With this current controller, the current control performances can be remarkably improved, since the current slopes are directly controlled by an optimal manner. The block diagram of a proposed three-level predictive current controller is shown in Fig. 2.

## 5 Simulation and Discussion

The typical responses of the proposed three-level predictive current control technique are comparatively investigated with other types of the current control techniques. The parameters used in the simulation Fig. 3 and 4 are as follows:

$$V_s(t) = \sqrt{2} 100 \sin(120\pi t), \quad L_s = 100\mu H, \quad C_s = 500\mu F, \quad R_L = 50\Omega, \\ f_s = 100kHz, \quad I_{COM} = V_s(t)/5, \quad L_f = 27\mu H, \quad R_f = 2\Omega, \quad C_f = 47\mu F$$

By using the proposed sampled data modeling, the average value of the rectified line current  $i_{s,ave}$  are shown in Fig. 3 for the various current control techniques with arbitrary current command. In this simulation, the control performances of Fig.3 (a) and (b) are generally shown to be undesirable with respect to current ripple. It is very difficult to obtain an optimized response in the sense of reduced current ripple since the control variable  $s^*(k+1)$  is not directly controlled in these techniques. As can be seen in this figure, the proposed three-level predictive current control technique shows the better performance than those of the other control techniques with respect to the line current harmonics. Furthermore, the current is increased continuously before reaching neighborhood of the current command, and then less steep current slopes are utilized. Thus, fast transient response can also be obtained. The proposed current control technique and a conventional predictive and a bang bang control techniques are simulated as shown in Figs. 4. As can be seen

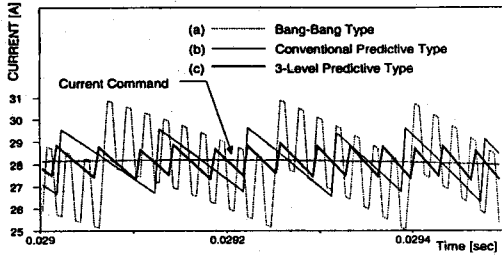
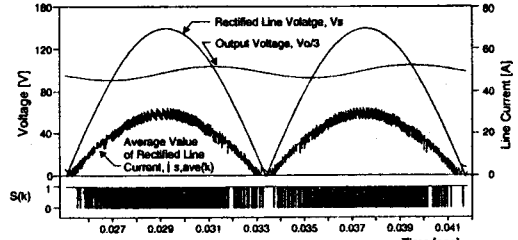


Fig. 3 Average Value of Rectified Line Current  $i_{s,ave}$  for the Various Current Control Technique

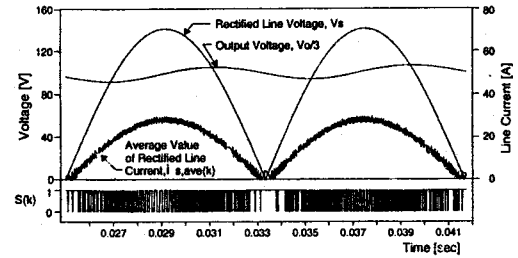
in these figures, the current control performance with respect to line current harmonics is notably improved by using the proposed control technique. Thus, it can be considered that the proposed three-level predictive current controlled PP-QSRR are very useful for power factor correction applications.

## 6 Conclusions

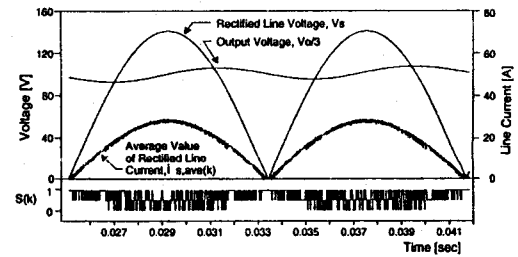
In this paper, a new three-level PP-QSRR for the unity power factor operation is presented. The zero current switching operation of the converter allows a substantial reduction in size and weight as compared to the conventional power factor improvement techniques. The sampled data dynamic modeling and three-level predictive current control technique are also proposed to perform the analysis and to improve waveform quality of the line current. Due to the many advantages including the high efficiency, ZCS, ease of



(a) Bang Bang Type Current Control Technique



(b) Predictive Current Control Technique



(c) 3-Level Predictive Current Control Technique

Fig.4 Simulation Results for the Various Current Control Techniques

control, linear characteristics like those of the conventional PWM converter, and low EMI, the proposed circuit, proposed modeling, and the current control technique are expected to be useful for the power factor correction.

## 7 References

- 1 MANIAS, S., and ZIOGAS, P.D.: 'An SMR topology with suppressed DC link components and predictive line current wave shaping', IEEE Industry Application Society Annual Meeting, 1986, pp.630-639
- 2 SEBASTIAN, J., UCEDA, J., COBOS, J.A., and GIL, P.: 'Using zero-current-switched quasi-resonant converters as power factor preregulator', IEEE Industry Elect. Conf., 1991, pp.225-230
- 3 DONCKER, R.W., and VENKATARAMANAN, G.: 'A new single phase AC to DC zero voltage soft switching converter', IEEE Power Elect.Spec.Conf., 1990, pp. 206-212
- 4 KO, J.H., HONG, S.S., ANN, T.Y., and YOUN, M.J.: 'Dynamic modeling and current control technique for quantum series resonant converter with non-periodic integral cycle mode', International Journal of Electronics, 1991, pp. 885-897
- 5 MOON, G.W., JO, B.R., AHNN, H.W., and YOUN, M.J.: 'Modeling and predictive current control technique for new zero-current switched high power factor rectifier', IEEE International Symposium on Industrial Electronics, 1993, pp. 498-502